Comparison Between Two Wind-Optimal Strategic Flight Plannings for North Atlantic Traffic

Imen Dhief, Daniel Delahaye, Nour Elhouda Dougui, Olga Rodionova

Comparison between two wind-optimal strategic flight plannings for North Atlantic traffic

Imen Dhief* and Daniel DELAHAYE†
French Civil Aviation University(ENAC) 7 avenue Edouard Belin, 31400 Toulouse, France,

Nour Houda Dougui‡
Heterogeneous Advanced Networking and Applications Research group ENSI, 2010 Manouba, Tunisia

Olga Rodionova§
Innov'ATM, 15 rue Alfred Sauvy, 31270 Cugnaux, France

The North Atlantic oceanic airspace is considered the most congested oceanic airspace in the world. For many years, air traffic control in this airspace has experienced difficulties due to the limited radar coverage. To support conflict-free flight progress, a structure of routes, called Organized Track System, is established in the North Atlantic airspace and very restrictive separation standards are applied. The development of the Automated Dependent Surveillance-Broadcast system provides an opportunity to improve the flight planning operations over the oceans by reducing separation norms.

The aim of this study is to improve the traffic efficiency in the North Atlantic airspace by developing new approaches to organize the transatlantic traffic at the strategic level. The first considered approach proposes a new route structure, referred to as Wind-Optimal Track Network, to replace the Organized Track System, while the second one is based on Wind-Optimal Free Routes. The problem is modeled as an optimization problem and resolved further via Simulated Annealing combined with Sliding Window algorithm. Results of simulations performed on the real traffic data prove that about 76% of flights decreased their cruising times by more than half an hour when flying wind-optimal tracks rather than using their great circle routes from the departure to the destination. Furthermore, by comparing the two proposed methods we conclude that Wind-Optimal Free Routes implies lower cruising times, while the Wind-Optimal Track Network is much more robust under changing wind fields.

*PhD student, MAIAA-ENAC, imen.dhief@recherche.enac.fr.
†Associate Professor, MAIAA-ENAC, Daniel.Delahaye@recherche.enac.fr.
‡Reasercher, HANA-ENSI
§Research engineer, Innov'ATM

Introduction

The North Atlantic oceanic airspace (NAT) is considered to be the most congested oceanic airspace since it connects two densely-populated areas i.e. Europe and North America. According to [1], there are currently about 1000 flights that cross the NAT daily and the traffic density is steadily increasing. For example, the International Air Transport Association (IATA) statistics estimated that the traffic growth over the NAT airspace was about 4.8% more in 2015 in comparison with 2014. Due to the passenger demand and time zone differences, air traffic in the NAT is concentrated within two major opposite-directional flows: the westbound flow departs from Europe in the morning and has the peak traffic crossing the $30W$ longitude between 1130 Coordinated Universal Time (UTC) and 1900 UTC; the eastbound flow departs from North America in the evening and has the peak traffic crossing the $30W$ longitude between 0100 UTC and 0800 UTC.

In addition to this, aircraft operating in the NAT are subject to very strong winds induced by the jet streams. Jet streams are fast air currents forming a tube in the upper atmosphere, typically between $20,000$ and $50,000$ feet and running mainly in east direction, with an average speed around 100 kts and up to 200 kts. Ideally, eastbound flights would prefer to exploit the jet stream strong tailwind, while westbound flights would rather avoid the jet stream headwinds. As a result, the traffic demand becomes highly concentrated within the two flows. Finally, most part of the NAT suffers from the lack of surveillance, which means that flights cannot be tracked by the traditional radars. It is therefore crucial to establish safe, robust and optimal procedures in order to organize this huge traffic volume.

Nowadays, in the conditions of limited surveillance, this problem is solved by introducing a system of pre-defined tracks referred to as the Organized Track System (OTS).

The OTS is created independently for eastbound and westbound traffic, taking into account the position of the jet streams, to accommodate as many flights as possible close to their minimum-time tracks and altitude profiles. Each OTS includes between 5 to 7 nearly parallel tracks spread within flight levels from Flight Level (FL) 310 to FL390. About 10 way-points are fixed in each track.

Currently, about half of the NAT traffic utilizes the OTS [1]. A flight that plans to operate on OTS tracks has to submit a flight plan to the corresponding Oceanic Area Control Center (OACC) specifying the desired track, desired step climbs and Mach changes, estimated track entry time and the entry time in the Oceanic Flight Information Region (FIR) boundaries. Furthermore, operators are required to indicate their aircraft and crew capabilities in the flight plan. Such information allows Air Traffic Control (ATC) to apply appropriate separation criteria to the flight.

In real-time operations, all OTS flights should operate on great circle joining OTS track way-points at predefined FL and at constant predefined Mach. The planned Mach and FL for the OTS track should be requested from the concerned OACC at the last domestic reporting point prior to NAT entry and the assigned

FL and Mach must be delivered via the clearance response while the aircraft is within radar coverage.

Within the NAT, pilots are required to request ATC approval for any en-route FL or Mach modification. Such modifications can be approved by ATC or denied depending on potential traffic conflicts. Furthermore, FL and Mach changes are only allowed at way-points. Pilots can request also re-routing between tracks. However, such requests often get rejected from the safety perspective because of the large separation norms.

Separation norms refer to the minimum distance that must be kept apart between aircraft operating in controlled airspace and are typically defined for vertical, lateral and, in some cases, longitudinal separation. As in a non-radar environment aircraft position prediction is less precise, separation norms in oceanic airspaces are much higher than in the continental ones: lateral separation is extended to 60 NM (111.11 km), compared to 5 NM in continental airspace, and vertical separation is 1000 feet (304.8 m). The OTS is constructed to comply with these separation norms. In addition to this, once aircraft enter the OTS system, controllers have to ensure longitudinal separation which represents the hold time between two aircraft in the same track. Nowadays, the longitudinal separation is 10 minutes between two aircraft in the same track and becomes 15 minutes if an aircraft changes its track. The three aforementioned separation standards are presented in Figure 1.

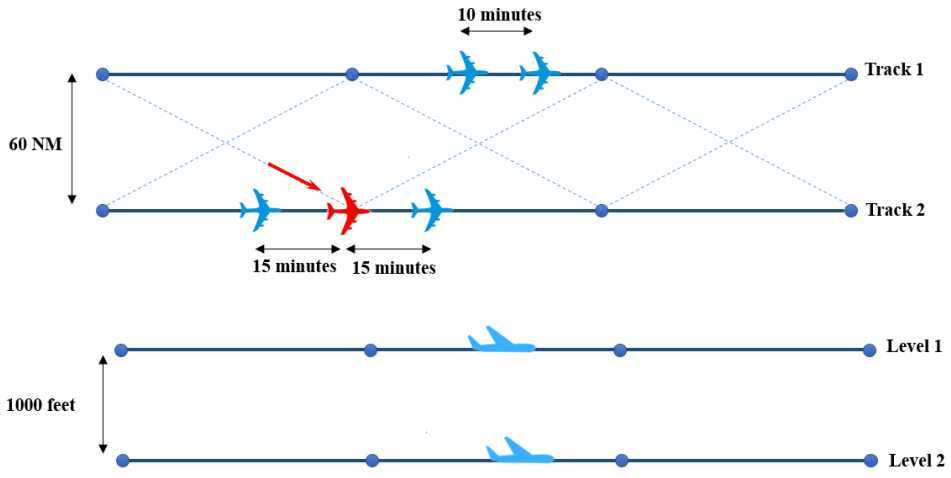

Fig. 1 Separation standards in oceanic airspace

These rigid rules limit the efficiency of NAT airspace, and the efficiency of each single flight as well. In fact, the OTS structure reduces the number of flights authorized to cross the NAT at a given time. As a result, flights are penalized with huge delays and deviations from desired trajectories (horizontal and vertical). This situation induces additional congestion in the post and/or pre-oceanic continental airspace.

Furthermore, given that the width of the jet stream is 50 to 100 NM, only one or two OTS tracks can

really benefit from the wind direction. As each flight would prefer to follow the track with preferable wind, the traffic concentration along such tracks is increased, which becomes an issue regarding the NAT traffic growth. Thus, the question arises of whether the OTS is the best way to organize the NAT traffic in the future.

Reduction of the separation norms makes it possible to exploit different ways of organizing traffic, alternative to the OTS. Recently, reduction in oceanic separation norms has been widely discussed in order to prove its feasibility. For instance, in 2015, the reduced lateral separation minima (RLatSM) equal to 25 NM was introduced in NAT by establishing one-half-degree spacing between the OTS center tracks between FL350 and FL390 [1]. Furthermore, in [2], authors affirm that implementing a longitudinal and lateral separation of 10 NM in oceanic airspace is conceivable by increasing the data link performances in controller-pilot communication and surveillance. The communication and navigation performance requirements to allow the reduction of the separation norms are presented in the report of the flight safety foundation [3]. Therefore, in order to guarantee efficient traffic separation in the conditions of increasing traffic density, alternative means of communication, navigation and surveillance were developed and started to be implemented.

One of the most promising technologies is the Automatic Dependent Surveillance-Broadcast (ADS-B), which consists of ADS-B In and Out modules. ADS-B allows the aircraft to determine their positions via satellite navigation (Global Positioning System GPS). Then, each aircraft equipped with ADS-B Out can broadcast its own information (identification, position, velocity, etc.) which is received by both controllers and surrounding traffic, equipped with ADS-B In. Thus, ADS-B allows air traffic controllers tracking aircraft in real-time almost anywhere in the world, and at the same time it provides nearby appropriately equipped aircraft with situational awareness and allows self separation. Thanks to the joint capabilities of ADS-B In and ADS-B Out, ATC is able to supervise and separate aircraft with improved precision and timing. For this reason, a significant reduction in the separation standards can be achieved.

There are two important works aimed at financing, developing, deploying and operating solutions for tracking and monitoring aircraft anywhere in the world by using ADS-B. [3]:

- A joint working group made up of Nav Canada *, UK NATS † and Air-services Australia representatives;
- State Aviation System Plan (SASP) work-group.

The resulting research and analysis anticipates lateral and longitudinal standard of 15 NM when using ADS-B combined with existing communication systems. The SASP advice suggests that mathematical modeling and validation can confidently be completed by 2018 [3, 4]. However, this reduced separation is not yet approved by the International Civil Aviation Organization (ICAO) [5]. So far, the Federal Aviation Administration

*NAV CANADA is a private, non-share capital corporation that owns and operates Canada's civil air navigation service (ANS).

†NATS is the UK's leading provider of air traffic control services.

(FAA) estimates that the equipage rate of ADS-B Out on NAT flights will be 83% in 2018, 95% in 2019, and will reach 100% by January 1, 2020 [6]. Nevertheless, ADS-B In is not mandated yet.

Taking into account the existing limitation, we made the following assumptions in the current work:

- Longitudinal separation is decreased from 10 minutes to 2 minutes between consecutive aircraft on the same track, and from 15 minutes to 3 minutes when the aircraft changes its track.
- Lateral separation of 12 NM when aircraft are following parallel track and re-routing between these tracks is not allowed. Otherwise, the lateral separation is 30 NM.

In this paper, we propose efficient flight schedules that benefit from the wind direction and satisfy the considered separation between the flights. That is done at a strategic level, i.e. several hours or days before real time operations, in order to facilitate the controller workload during the tactical phase. To deal with this problem, two different approaches are presented: the first one proposes a new, more efficient, route structure, called Wind-Optimal Track Network (WOTN), to replace the OTS, while the second one assumes that Wind-Optimal Free Routes (WOFR) are operationally acceptable, and do not use any track network. The main challenge of the strategic planning is dealing with high level of uncertainty, resulting, in particular, from the wind prediction errors. Thus, robustness of the proposed solutions is crucial: we want to assure that the required separation is maintained for the proposed flight schedules regardless the changing wind conditions.

This paper is organized as follows: Section I gives a brief overview of the relevant works on optimizing air traffic in the oceanic airspaces. In section II, the problem formulation is presented and the input data of our problem are defined. Two approaches to the problem resolution, WOTN and WOFR, are discussed respectively in sections III and IV. Then, numerical results are compared in section V, followed by conclusions and perspectives.

I. Related work

Literature review revealed several methods for improving oceanic air traffic management. The first group of methods exploited the existing OTS structure under reduced separation norms. Williams et al. [7, 8] investigated potential benefits from implementing an Airborne Separation Assurance System (ASAS) In-Trail Climb (ITC) procedure, applied first to the South Pacific oceanic airspace(SOPAC) [7], then to the NAT [8]. Here, an aircraft was allowed, while climbing to a higher flight level, to apply an alternative longitudinal separation standard of 10 NM with an aircraft at an intermediate flight level (between the old and the new FL reached). This research revealed improvements in operational efficiency through fuel savings and additional cargo revenue potential and proved clearly that reducing the separation standards in oceanic airspaces may be beneficial. A study by Rodionova et al. [9] discussed potential benefit from optimizing the flight routes

within the OTS structure. The authors proposed to favor the track changing within the OTS which permits to reduce the total flight trajectory length, cruising time and fuel consumption. The authors formulated an optimization problem aimed at finding a conflict free trajectory set within the OTS represented as a grid of nodes and links and solved it using the Simulated Annealing (SA).

The same authors applied the Genetic Algorithm (GA) to resolve a similar optimization problem in [10] for the real flight data involving about 350 flights. Simulations showed that a conflict-free solution can be found only under the reduced separation norms which revealed benefits from operating the ADS-B. At the same time, these results demonstrated one of the important limitations of the OTS: the tracks are not all wind-optimal.

Another group of research methods studied the potential benefits of transitioning from the route structure to wind-optimal routes. Multiple studies, for instance [11–13], looked for the benefits from flying wind-optimal trajectories in the continental airspace. However, to our knowledge, very few publications discussed this problem for the oceanic airspace. In fact, wind-optimal trajectories applied in continental airspaces are hardly implemented in oceanic airspace due to the large separation norms and to the lack of radar coverage. With the recent introduction of ADS-B, it is conceivable to allow oceanic flights to follow more flexible and optimal routes. Generally, generating optimal aircraft trajectories involves not only flight and air traffic performances but also meteorological conditions. Therefore, the first important step to perform in order to construct wind-optimal trajectories consists of analyzing the weather particularities of the considered airspace.

A detailed analysis of meteorological conditions, including a classification of weather patterns in NAT airspace, our region of interest, was presented in [14]. The climate cost functions were calculated, for each weather pattern, by selecting representative days in both winter and summer. Analysis of climate impact from NAT flights was conducted in terms of CO_2 and O_3 emissions, water vapors and contrails. Authors concluded that climate impact was more important for long flights, and thus, affirmed the importance of selecting wind-optimal trajectories, in particular, for NAT flights.

In [15], authors applied the Dynamic programming to generate wind-optimal flight routes for Central East Pacific flights and revealed an average time and distance savings of 9.9 minutes and 36 nmi per flight, respectively.

In [16], authors presented an approach for cross-polar aircraft trajectory optimization and analyzed its potential climate impact. The research focused on deviating flights from fixed routes to operate on wind-optimal routes in order to reduce environmental emissions by minimizing fuel burn. Wind-optimal flight trajectories were generated by applying Pontryagin's Minimum Principle [17]. The study revealed a reduction of almost 0.3% to 2% in fuel consumption when following wind-optimal trajectory compared to great circle route for cross polar flights.

The same approach was applied in [18] in order to generate wind-optimal trajectories in cruise for NAT flights. The 2D-horizontal trajectory was optimized by determining the heading that minimizes travel time in the presence of wind. Results along the entire month of July 2012 showed mean fuel savings of 2.4% and 2.2% for the eastbound and westbound flights respectively comparing to the flight routes following the NAT OTS.

The use of wind-optimal routes, being very beneficial especially in terms of fuel savings, generates a large number of potential conflicts between flights. As a result, the NAT becomes extremely congested. Some recent works aimed to de-conflict wind-optimal routes over the oceanic airspace. In [19], the authors presented a conflict-detection approach, which was based on the Conflict Grid where each grid cell can be occupied by only one aircraft at any time. In this study, the problem of conflict resolution was formulated as a job-shop scheduling problem. The approach was applied to deconflict wind-optimal trajectories for Central East Pacific flights generated in [15]. The flight departure times were considered as the only optimization variables. The advantage was that the resulting aircraft trajectories remain wind-optimal as their shapes are not changed. However, the resulting solution may involve very large flight delays which is an important issue from the operational point of view.

In [20] a method for detecting and resolving conflicts between wind-optimal flight trajectories in the NAT airspace at strategic level was introduced. The conflict resolution was ensured by a SA algorithm and was based on two maneuvers: changing the departure time, and slightly modifying the geometrical shape of the trajectory while remaining wind-optimal. More details and results about the adopted approach are further presented in [21]. Findings showed that an important reduction in the number of conflicts can be achieved while keeping flight trajectories as close as possible to wind-optimal ones. However, the robustness of the resulting trajectories under variable winds was not assured by this approach.

An innovative approach to optimize oceanic air traffic was presented in [22]. The authors applied the "Flocking Boid" model in order to construct conflict free trajectories for NAT eastbound flights. Here, authors relied on two particular behavior of the NAT flights to implement their model. First, within NAT flights, the problem of intersecting flights was not confronted as eastbound and westbound traffic are treated separately. Second, eastbound aircraft share a long distance of their flights inside the NAT region as they prefer to follow the jet stream tailwind. Furthermore, assuming that all aircraft are equipped with ADS-B In and Out systems, each flight can share its information with neighbour flights, and get the information about the surrounding traffic as well. The idea of the method was to simulate the NAT eastbound flight flow as the bird flow, moving in the same direction and aiming to travel the optimal trajectories while avoiding conflicts between each other. Due to the specificity of the considered problem, the "Flocking model" was adjusted and new rules were included in order to avoid the sinuous behaviour of trajectories and to assign to aircraft different destinations. The computational results proved a considerable reduction in the number of conflicts

with reasonable delays and elongation from the direct path. However, the robustness of these trajectories under strong and variable winds remained a serious issue.

II. Problem Statement

This work is aimed at proposing a new solution for organizing the traffic within the NAT instead of the OTS taking advantage of the optimal wind directions and assuring that the required separation norms are maintained. The simulations were performed for the NAT flight schedules over the month of July 2012. These data were obtained from the flight tracks recorded by EUROCONTROL's Network Manager and the FAA's Enhanced Traffic Management System (as described in [18]) and made available for this research by NASA Ames Research Center. Due to the similarity of the obtained results, in this paper, only the results for eastbound flights on July $15th$ 2012 are presented. Further in this section, we discuss the problem statement and present the input data.

A. Flight data

The flight set consisted of 546 flight. The flight data was obtained from the submitted flight plans for the transatlantic flights. The features of these flight plans which are relevant to this study are:

- Origin and destination airports;
- Desired departure time;
- Entry and exit points in the NAT airspace;
- Desired flight level;
- Desired true airspeed.

Considering these data, flight trajectories are constructed in a specific way for each of the two considered approaches, namely WOTN and WOFR. For the purpose to simplify the simulations, the following assumptions are made.

- We consider the desired aircraft speed to be constant for the entire trajectory in this study. This assumption is rational, as we are tackling only the en-route phase of flights in the NAT. In fact, flights tend to maintain constant speed while following an OTS track, since it guarantees the optimal fuel consumption, whereby we assume that flights keep the same speed profile even when they do not use the OTS.
- We assume, for simplicity, that flight levels are constant for each flight and do not change for the entire trajectory.
- We treat only eastbound traffic. As concluded in the Introduction, the eastbound and westbound traffic flows are mainly separated in time, due to passenger demands and time zone differences, and laterally,

due to energetic nature of the minimum-time flight routes resulting from the natural atmospheric conditions. In addition to this, as from the current operational procedures, the eastbound flights mainly occupy odd flight levels (ex. FL350, FL370), while the westbound flights are scheduled at even flight levels (ex. FL340, FL360); thus, the flows are basically separated vertically as well. Taking these features into account, we can assume that flights within the opposite-directional flows never interact with each other and can be considered independently.

B. Wind data

The wind data is obtained from the GRIdded Binary (GRIB) files created by the meteorological centers (National Oceanic and Atmospheric Administration (NOAA), Meteoblue, The Fleet Numerical Meteorology and Oceanography Center (FNMOC)) and available online [23]. This data is then converted into a 3-

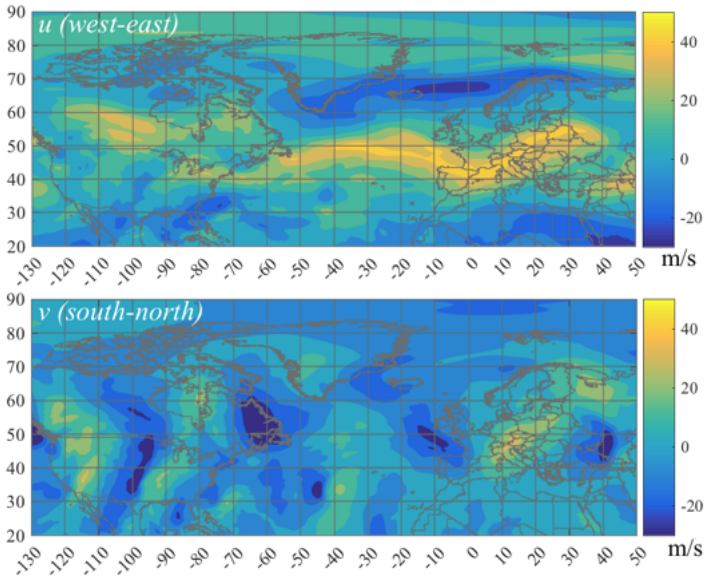

Fig. 2 Forecast wind field on July 15^{th} 2012 at 0000 UTC at FL370: W_u-component (top) and W_v-component (bottom), in meters per second (m/s)

dimensional grid covering the world airspace, where each grid cell has the horizontal dimension of $(0.5^\circ \times 0.5^\circ)$ and vertical dimension of 1000 feet (one flight level) and contains W_u (west-east) and W_v (south-north) wind components. Each such grid corresponds to a particular hour of the day, with a 6-hour time horizon. Figure 2 shows an example of a wind field on July 15^{th} 2012 at 0000 UTC at FL370, extrapolated from the wind components at the grid cells (W_u-component on top, and W_v-component on bottom).

In addition to the nominal forecast wind field obtained from GRIB files, we want to consider uncertainty in wind prediction, in order to verify the robustness of the proposed solutions. Similar to numerous related studies, for instance [24–27], we introduce wind uncertainty via wind scenarios. Five wind scenarios are

considered in this paper, referred to as $s0$, $s1$, $s2$, $s3$ and $s4$, where $s0$ corresponds to the nominal forecast wind for the current day, and other scenarios are constructed as a combination of forecasts from the previous, current, and the next day (refer to [28] for more details). Figure 3 shows such scenarios for W_u-component (most meaningful for transatlantic flights) on July 15^{th} at 0000 UTC at $FL370$ within the NAT.

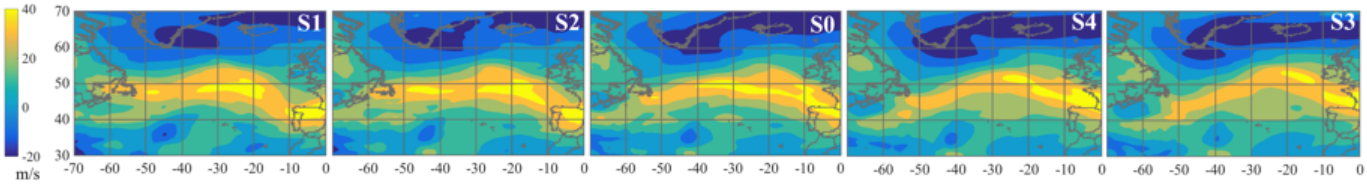

Fig. 3 Five forecast scenarios for W_u (east-west) wind component over NAT on July 15^{th}2012 at 0000 UTC at $FL370$

C. Problem statement

Our problem can be formulated as follows. We are supposed to be given:

- Original flight schedules based on the submitted flight plans,
- Forecast wind fields,
- Separation norms.

We would like to assign to each flight a trajectory to follow using one of the traffic organization methods:

- Based on the WOTN structure (as discussed in Section III), or
- Based on wind-optimal free routes (WOFR) (as discussed in Section IV).

Our main goal is to resolve all potential conflicts between such trajectories, while maintaining optimal routes in terms of flight cruising times. In ATC, the term *conflict* refers to the violation of the established separation norms. As mentioned in the Introduction, we consider reduced oceanic separation norms assuming that all aircraft are equipped with ADS-B. Conflict detection based on the given norms is discussed independently for the two traffic organization methods in Sections D and B. For the purpose to simplify the simulations, we concentrate our effort at conflict detection and resolution within the NAT only, as it is the main subject of the study. We omit the possible conflicts in the continental airspace which may be induced by our solution, considering that they are easier to resolve thanks to the relatively small continental separation norms. Thus, we end up with a conflict detection and resolution problem. Sections III and IV propose two solutions to this problem, and Section V discusses the obtained results.

III. Problem formulation and resolution via a new Wind-Optimal Track Network (WOTN)

In this section, a new route structure for the NAT is proposed, referred to as Wind-Optimal Track Network (WOTN). The construction of WOTN represents an improvement of the actual OTS that is based on two major factors. First, this WOTN allows eastbound flights to follow the jet stream direction which is beneficial for the en-route fuel consumption. Second, assuming that all aircraft are equipped with ADS-B In and Out, reduced separation norms are considered.

A. WOTN construction

In this section, we present the new WOTN which we use instead of the OTS to schedule transatlantic flights. As mentioned in the Introduction, OTS tracks are separated by 60 NM, however, in WOTN, we keep tracks separated by 12 NM. This reduction is reasonable since we are interested in aircraft equipped with ADS-B system. We consider the portion of airspace between longitude $-90°$and $10°$, and latitude $30°$and $70°$, which represents the NAT. As shown in section B, jet stream is mainly concentrated around latitude $50°$. First, we construct entry points of the new tracks for eastbound flights: at longitude $-70°$, we put virtually 8 points equally distributed, starting from latitude $42°$and separated by $120NM$. Exit points are constructed similarly at longitude $-10°$. Then, starting from the entry point at each track, we merge all tracks to the center (around latitude $50°$), and we keep tracks parallel and separated by $12NM$ along $1600NM$ (this part of the WOTN is referred to henceforth as "parallel track section"). Finally, each track joins the corresponding exit point. Figure 4 illustrates the WOTN tracks in the presence of strong winds caused by jet streams.

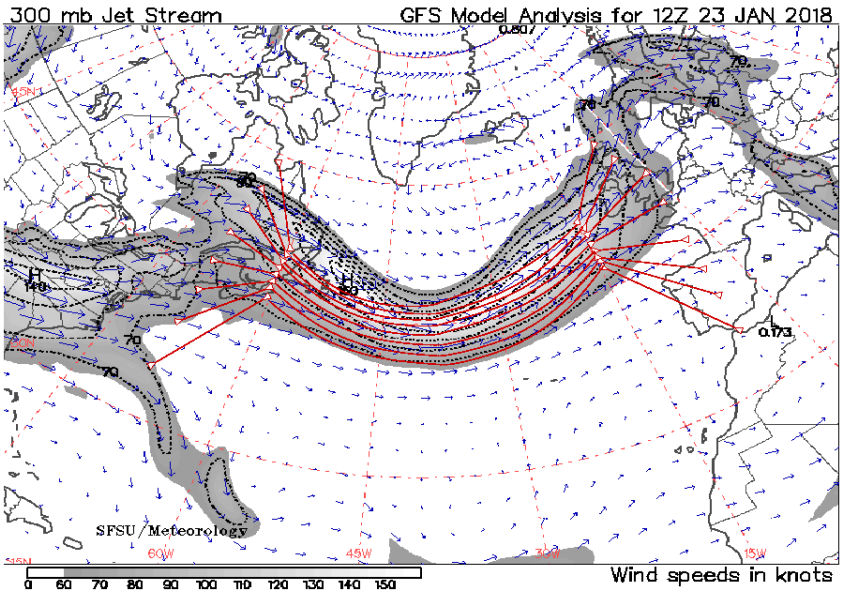

Fig. 4 WOTN tracks in the jet streams

WOTN tracks are in red color. The parallel track section is completely merged within the jet stream and follows its shape.

Within the parallel track section, we do not allow aircraft to change their tracks: an aircraft entering the parallel track section has to keep its track up to the exit point of this section. However, as aircraft may desire to enter and exit the NAT at different tracks, we want to guarantee reliable transitions between the tracks. Thus, sections before and after the parallel track section are considered as filters, where each track contains a number of way-points. Flights are allowed to change their tracks only at these way-points. Thus, our WOTN is defined by a set of way-points connected with links. It can be modeled with a grid with N_y tracks where each track contains N_x way-points and N_z flight levels. Figure 5 illustrates the grid model in horizontal dimension.

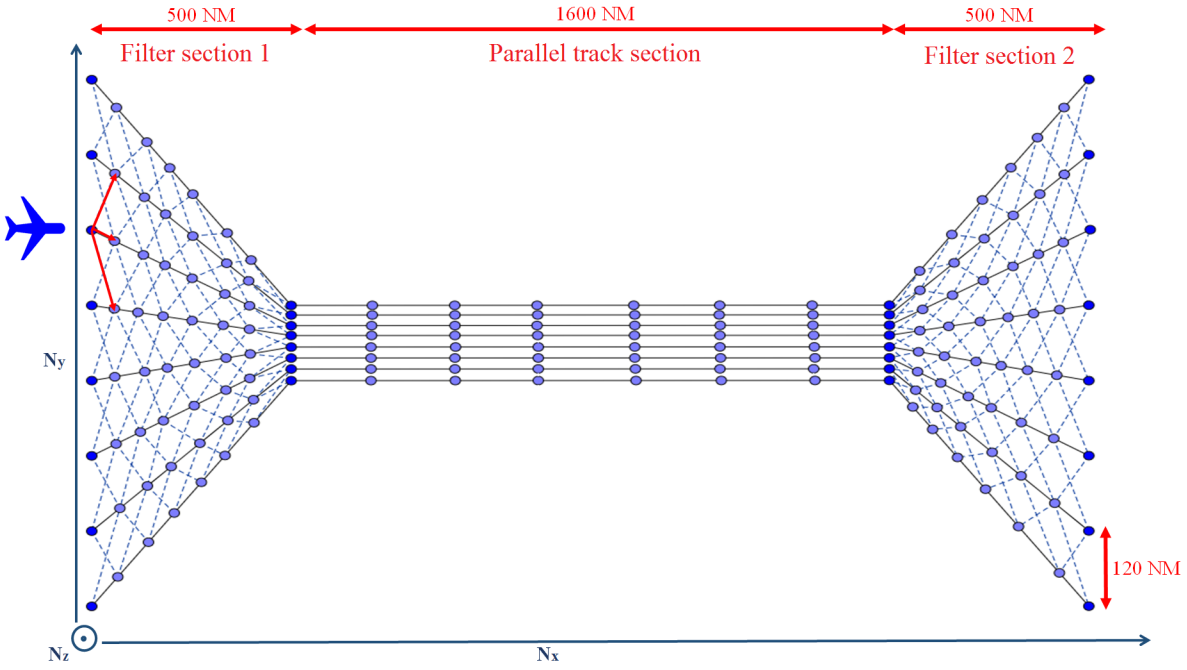

Fig. 5 Horizontal section of the WOTN grid model

B. Flight maneuvers

For each flight f, we represent the input data presented in Section A as follows:

- ${T_{In}}^f$ the desired track entry time,
- ${Track_{In}}^f \in 1, 2, \ldots, Ny$ the desired entry track which represents the closest track to the departure airport,
- ${Track_{Out}}^f \in 1, 2, \ldots, Ny$ the desired exit track which represents the closest track to the destination

airport,

- FL^f the desired flight level,
- V^f the desired flight airspeed.

In the current work, we assume that the desired flight level (FL^f) is fixed for each flight and remains constant for the entire trajectory. This assumption is made in order to simplify the comparison between the proposed methods further. Nevertheless, flight level change is highly recommended for oceanic flights in order to follow their optimal vertical profile. Such a maneuver can be easily implemented inside the WOTN by allowing climb at way-points. Furthermore, the aircraft airspeed (V^f) is also fixed and remains constant for the entire trajectory, while other parameters may be changed in order to find a conflict-free solution. Thus, entry delay less than 20 minutes is allowed. Moreover, the entry and exit track restrictions are relaxed by allowing aircraft to enter and/or exit an adjacent track. Thus, we define the following decision variables:

- ${ATrack_{in}}^f = {Track_{In}}^f + / - 1$ the assigned entry track.
- ${ATrack_{out}}^f = {Track_{Out}}^f + / - 1$ the assigned exit track.
- ${D_{in}}^f \in [0, 20min]$ the time delay at the entry point.

As mentioned in the Introduction, when an aircraft enters a predefined track at a predefined flight level, it is required to follow the same track and flight level unless a maneuver is done. In WOTN, such maneuvers can only be executed at way-points of the filter sections. At each such way-point, a flight has three alternative maneuvers available: either it continues along the same track or it moves to an adjacent one (northern or southern). We model these maneuvers with the following decision variables:

$$ {X_i}^f = \begin{cases} 1 & \text{if the flight switches to the northern adjacent track at the waypoint i} \\ 0 & \text{if the flight continues along the same track} \\ -1 & \text{if the flight switches to the southern adjacent track at the waypoint i} \end{cases} \tag{1} $$

where $i \in \{1, 2, ..., N_x - 1\}$ represent the way-points where a rerouting from one track to another is possible, i.e. the way-points of the filter regions.

C. Flight time computations in wind fields

To simulate flight trajectory, we need to compute for each aircraft the times of passing the way-points that depend on aircraft true airspeed and the wind direction and speed which are given data in our problem. To do so, we calculate the wind vector at each way-point of the WOTN using a grid of wind data (described in Section B). For each way-point WP_i given by its spherical coordinates (ϕ_i, λ_i, h_i) (latitude, longitude and altitude), we extract the east wind component W_u and the north wind component W_v and calculate the wind

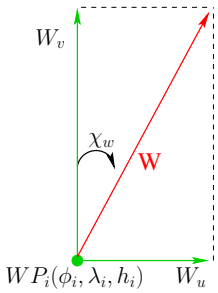

Fig. 6 Wind information in each Way-Point (WP_i)

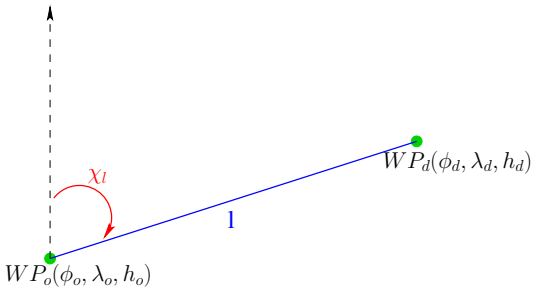

Fig. 7 The link bearing angle

norm $||\overrightarrow{W}|| = \sqrt{W_u^2 + W_v^2}$ and the associated wind bearing $\chi_w = arctan(W_u/W_v)$ (see Figure 6).

To be exact, the time needed by the aircraft to fly along each link is calculated as follows:

$$t = \frac{d_l}{V_g} \tag{2}$$

where

$$V_g = V^f \sqrt{1 - (\frac{V_w}{V^f})^2 sin^2(\chi_{wg})} + V_w cos\chi_{wg} \tag{3}$$

V^f is the flight airspeed, V_w is the magnitude of the wind velocity vector, V_g is the ground speed, χ_w is the wind heading, χ_g is track heading and χ_{wg} is track relative wind heading. As the flights within WOTN mainly follow the jet stream, the tail wind component of the wind vector is much greater than the crosswind component for such flights, so the last one can be omitted in order to simplify the calculations without much impact on the results. These assumptions has been introduced in [29]. This gives the following simplifications:

- we assume that the wind vector has the same heading as the considered link. Thus, $\chi_w = \chi_g$ and $\chi_{wg} = 0$;
- we assume also that the magnitude of the wind velocity vector consists only of the tail wind TW.

This results on the following simplified equations:

$$V_g = V^f + V_w = V^f + TW \tag{4}$$

$$t = \frac{d_l}{V^f + TW} \tag{5}$$

To compute the tail wind for each link, let (ϕ_o, λ_o, h_o) and (ϕ_d, λ_d, h_d) be the spherical coordinates (latitude, longitude and altitude) of the link origin way-point WP_o and the link destination way-point WP_d respectively.

The associated bearing χ_l (see Figure 7) of each link l is given by the following formula [29]:

$$\chi_l = arctan(\frac{sin(\Delta_\lambda).cos(\phi_d)}{cos(\phi_o).sin(\phi_d) - sin(\phi_o).cos(\phi_d).cos(\Delta_\lambda)}) \tag{6}$$

where $\Delta_\lambda = \lambda_d - \lambda_o$. Then, the tail wind at each extremities of the link TW_o and TW_d is given by:

$$TW_o = ||\overrightarrow{W_o}||.cos(\chi_l - \chi_{w_o}) \tag{7}$$

$$TW_d = ||\overrightarrow{W_d}||.cos(\chi_l - \chi_{w_d}) \tag{8}$$

We associate to each link l the average of these two tail winds:

$$TW_l = \frac{TW_o + TW_d}{2} \tag{9}$$

Finally, the time needed by a flight to reach way-point WP_d from way-point WP_o can be deduced by:

$$t = \frac{d_l}{V^f + TW_l} \tag{10}$$

where d_l represents the length of the considered link along the great circle and V^f is the true airspeed of the aircraft.

D. Conflict detection strategy

As mentioned in section III-A, our WOTN is built in such a way as to satisfy the reduced separation norms: tracks are separated by 12 NM, flight levels are separated by 1000 ft. Thus, we only have to assure the longitudinal separation. It is assumed to be 2 minutes if aircraft are in the same track, and 3 minutes when an aircraft changes its track. Figure 8 shows the longitudinal separation norms.

Considering our WOTN, we either detect a conflict at nodes or at links. Conflicts at nodes are detected by sorting flights passing through a given node according to their arrival time and computing the difference in arrival times between each two successive flights in the sorted list. A conflict is detected when this difference is less than the longitudinal separation. Since each link is delimited by two nodes, we can detect conflict at links by comparing the sequence order of aircraft at the entry and exit nodes of a link. If there are two swapped flights, then an overtaking conflict is detected.

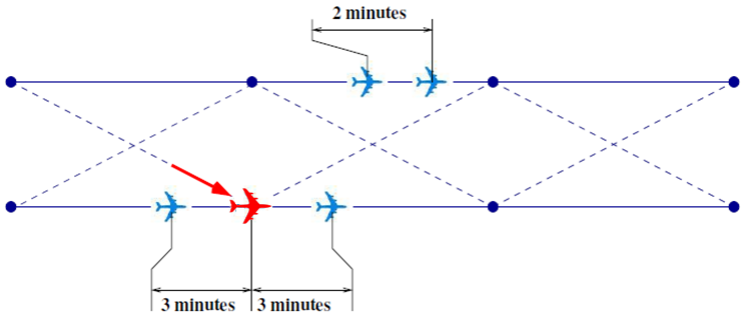

Fig. 8 Longitudinal separation norms

E. Objective function

Our goal is to generate a set of optimal trajectories for *Nb* eastbound flights while satisfying several constraints. There are different route optimality criteria such as total trajectory length, flight duration and fuel consumption. In this study, we choose to minimize the total cruising time since it is directly related to the fuel consumption. Although we have relaxed several flight parameters, we would like our proposed solution to satisfy the airline preferences as close as possible. Thus, we add the total delay and the cost of the deviation from the desired track to the objective function. Cruising time for each flight is the time needed to fly the sum of distances between the track way-points. Thus, total cruise time, C, corresponds to the sum of cruising times over all flights. Total entry delay, D, represents the sum of entry delays over all flights. The deviation delay for each flight represents required additional time to deviate from the desired track and reach the new assigned one. We get total deviation delay, R, by summing up deviation delays over all flights. The objective function, that we aim to minimize, is the weighted sum of these values as depicted in:

$$F_{obj} = d \times D + c \times C + r \times R \tag{11}$$

where the non-negative coefficients *(d,c,r)* are used to balance the three criteria according to the user preferences. The only physical constraints of the problem (except boundary constraints on decision variables) are conflict-avoidance constraints. We address these constraints by relaxation in the objective function. Therefore, we add the number of induced conflicts, C_t, to the objective function as the most important criterion to minimize. Ideally, we would like to reduce this number to zero. The objective function becomes then:

$$F_{obj} = C_t + a \times (d \times D + c \times C + r \times R) \tag{12}$$

where the coefficient a is added in order to give the highest priority to the conflict-free criterion. If all conflicts are resolved, the system continues to minimize the other criteria (cruising time, deviations and delays) while ensuring that the resulting solution remains conflict-free. Equation 12 can be also written as follows:

$$F_{obj} = C_t + d_1 \times D + c_1 \times C + r_1 \times R \tag{13}$$

where $d_1 = a \times d$, $c_1 = a \times c$ and $r_1 = a \times r$. In the computational result part, these parameters, namely d_1, c_1 and r_1 are empirically set and take different values in order to test their influence on the objective function results.

F. Optimization process

First, let us compute approximately the complexity of our problem. For each flight f, the introduced decision variables can take the following values:

- from 0 to 20 minutes of delay.
- 3 possible entry tracks and 3 possible exit tracks.
- 6 track changes on average chosen among the 14 waypoint positions (= 3003 options per flight)
- This gives more than $540,000$ options per flight.

If we consider 500 flight, we have $540,000^{500}$ options. Therefore, we are dealing with a highly combinatorial problem. We thus appeal to the stochastic optimization methods to tackle this problem. We start with pre-processing the flight set using a Sliding Window (SW) method. The latter consists in dividing the problem into a set of sub-problems. Then, each sub-problem is treated separately and sequentially via a Simulated Annealing (SA) algorithm.

The application of the SW method to our problem starts with sorting the flights according to their NAT entry times. Then, a time window interval of length T_w beginning at the earliest entry time is fixed. In each time window, four types of flight are identified:

- **Planned flights** are those that are planned to enter the WOTN after the time window.
- **Completed flights** are those that exited the WOTN before the time window.
- **On-going flights** are those that entered the WOTN before the time window and are still operating in the considered time interval.
- **Active flights** are those having the WOTN entry time in the considered time window.

Once the flight types are assigned to all flight, we proceed with the conflict resolution method. Planned and completed flights are not considered for the time window being treated. We apply the SA algorithm to fix the decision variables of the active flights while considering the on-going trajectories as constraints. Hence,

Table 1 Flight data

Flight	F1	F2	F3	F4
Departure time	10:00	10:40	11:35	12:15
Allowed departure time	[10:00, 10:20]	[10:40, 11:00]	[11:35, 11:55]	[12:15, 12:35]
Arrival time	12:00	13:00	14:20	15:00

Table 2 The first six iterations of the SW algorithm

SW iterations	1^{st}	2^{nd}	3^{rd}	4^{th}	5^{th}	6^{th}
Time interval	[10:00, 12:00]	[10:30, 12:30]	[11:00, 13:00]	[11:30, 13:30]	[12:00, 14:00]	[12:30, 14:30]
Active flights	F1, F2, F3	F2, F3	F3, F4	F3, F4	F4	$\emptyset$
On-going flights	$\emptyset$	F1	F1, F2	F1, F2	F2, F3	F2, F3, F4
Planned flights	F4	F4	$\emptyset$	$\emptyset$	$\emptyset$	$\emptyset$
Completed flights	$\emptyset$	$\emptyset$	$\emptyset$	$\emptyset$	F1	F1

the decision variables of on-going flight are not modified. At next iteration, we shift the time window by T_s (with $T_s < T_w$). This process is repeated until all flights are completed. Figure 9 illustrates a schematic example of the SW process. To give a numerical example, let us consider 4 flights $F1$, $F2$, $F3$ and $F4$.

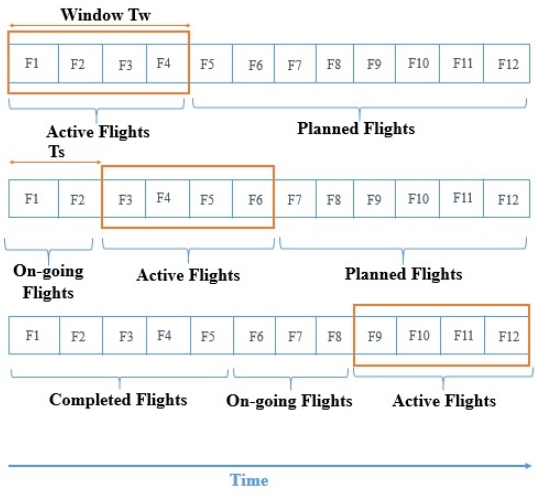

Fig. 9 Sliding window algorithm

Departure and arrival times of the considered flights are represented in the table 1. The allowed departure time in the table 1 represents the allowed delay for each flight. Let us consider the following settings: $T_w = 2$ hours and $T_s = 30$ minutes. The first six iterations of the SW are presented in Table 2.

Once a time window is defined with active flights identified and the on-going flight variables fixed, we apply the standard SA algorithm. The latter is a meta-heuristic algorithm inspired from thermodynamics [30, 31].

SA aims to minimize an energy function in the iterative process involving small changes to the current solution. The concept consists in accepting even the degrading solutions, but in a controlled manner. The process begins with a random solution and with a pre-determined control parameter T (called temperature). The latter decreases with the number of iteration. At each step, SA calculates a neighbor solution. It associates with each solution an energy value and probabilistically decides to keep either the neighbor solution or the current one. When T is large, exploration of the search space is promoted. When T is small, the system will converge towards the least energy solution. Flow chart representing SA process for heat up and cooling are presented in Figures 10 and 11, respectively. The SA algorithm is adapted to solve our problem as follows:

- The search space consists of all possible sets of flight trajectories. A solution is determined when we fix the decision variables for each flight in the flight set.
- The energy function represents the objective function of our optimization problem, as described in Section III-E.
- A neighbor solution is obtained by applying a local change to the current solution $\overrightarrow{x_i}$ in order to generate a new solution $\overrightarrow{x_j}$. It consists of changing one decision variable of an individual flight. The process of getting a neighbor solution is divided in two steps. First, we select a flight to be modified as being the one that generates the largest number of conflicts. Then, we select the decision variable to be modified. In order to satisfy aircraft preferences as much as possible, we consider a priority order when modifying flight decision variables. We attribute the highest priority to the en-route track change maneuver, since it does not affect much the trajectory length. Then, we consider modifying the entry/exit tracks. If a conflict-free solution does not exist, we delay the flight departure time.
- The acceptance probability of the neighbor solution $\overrightarrow{x_j}$ is given by $e^{(f(\overrightarrow{x_i})-f(\overrightarrow{x_j}))/T}$, where T is the temperature, $f(\overrightarrow{x_i})$ is the objective value of the current solution, $\overrightarrow{x_i}$, and $f(\overrightarrow{x_j})$ is the objective value of the neighbor solution, $\overrightarrow{x_j}$.
- The temperature decreases via a geometrical law given by $T_i = \alpha \times T_{i-1}$.
- The process stops when the temperature T goes below a predefined final temperature, T_f. T_f is adjusted to be: $T_f = \beta \times T_{Init}$ (with $\beta << 1$ and T_{Init} is the initial temperature).

The objective function is evaluated via a simulation process which requires a simulation environment. In such a case, the optimization algorithm controls the vector of decision variables, X, which are used by the simulation process in order to compute the performance (quality), y, of such decisions.

Usually, such a generation modifies only one component of the current solution. In this case, the vector $\vec{x}_i$ can be modified without being duplicated.

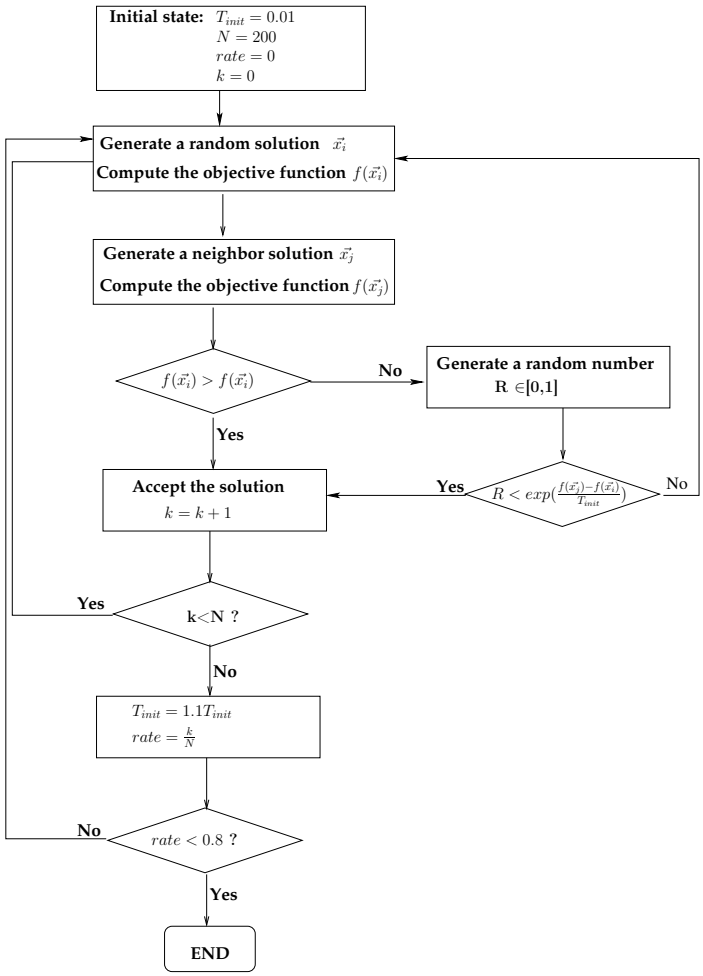

Fig. 10 Simulated Annealing: heatup

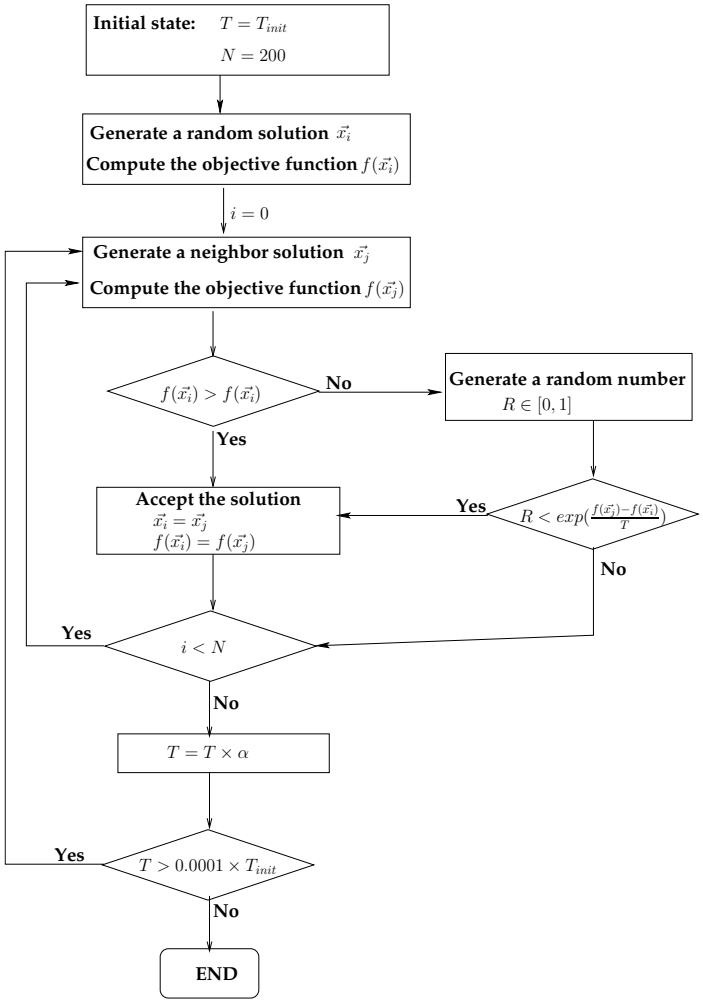

Fig. 11 Simulated Annealing: cooling

IV. Problem formulation and resolution via wind-optimal free routes (WOFR)

In this Section, we describe a method devoted to organizing the traffic in the NAT based on wind-optimal free routes (WOFR), which may become operationally acceptable thanks to more precise surveillance, reduction of the separation norms, and more efficient aircraft separation (including airborne self-separation) [32, 33]. The first step of the proposed method involves creating new aircraft routes for each single flight separately, taking into account aircraft performance metrics and environmental conditions. At the next step, the set of such trajectories is evaluated using required separation norms in order to detect potential conflicts. Finally, the trajectories are slightly modified in order to avoid these conflicts and guarantee conflict-free flight progress together with trajectory optimality.

A. Calculating WOFR

The problem of creating cost-optimal, wind-optimal, or climate-optimal routes has been addressed in many different ways in literature for decades [11, 14, 16, 18, 33–37]. The results of these simulations reveal significant benefits from flying such routes, in terms of time and fuel savings [16, 18], and emissions and contrails reductions [36, 37]. In this work, we use the approach based on the Pontryagin's Minimum Principle, discussed by Ng et al. in [16]. Following this approach, the wind-optimal trajectories are found by determining the optimal heading angle for aircraft during cruise, that minimizes the travel time in the presence of winds. In case of a constant altitude, the minimum-time trajectory is obtained by integrating aircraft equations of motion given below:

$$\dot{\phi} = \frac{V^f sin(\psi) + W_v}{R} \tag{14}$$

$$\dot{\lambda} = \frac{V^f cos(\psi) + W_u}{R cos(\phi)} \tag{15}$$

Here, ϕ is latitude, λ is longitude, V^f is airspeed, ψ is heading angle, R is the Earth radius. W_u is the east-component of the wind velocity, and W_v is the north-component of the wind velocity. The dynamic equation for the optimal aircraft heading is:

$$\dot{\psi} = \frac{-F(\psi, \phi, \lambda, W_u, W_v, V^f)}{R cos(\phi)} \tag{16}$$

where $F(\psi, \phi, \lambda, W_u, W_v, V^f)$ is aircraft heading dynamics in response to winds (see [16] for more details). Note that the minimum-time trajectory is also the minimum-fuel trajectory in this case. Thus, further in this paper, when addressing time savings, we mean that the fuel saving will be proportional. The resulting trajectory is represented as a sequence of 4-dimensional geographical points (ϕ, λ, h, t), where ϕ is latitude, λ is longitude, h is altitude and t is time (recorded with 1 minute interval).

In order to guarantee safe flight progress, we need to assure that the calculated WOFR remain conflict-free. For this purpose, a conflict resolution algorithm was developed [38], which permits to evaluate the number of potential conflicts for an arbitrary set of trajectories and to reduce this number by slight trajectory modification.

B. Conflict detection for WOFR

By the assumptions of this study, all transatlantic flights cruise at predefined flight levels, which guarantees vertical separation. However, horizontal and temporal separation remains the issue in the case of WOFR. We assume that the rational separation norms for the free flights in the NAT could be 30 NM for horizontal

separation, and 3 minutes for temporal separation (note, that a commercial aircraft cruising at the highest speed in 3 minutes would cover a distance equal to about 30NM). We adopted a point-to-point conflict detection method based on the 4-dimensional grid, which was first developed by Chaimatanan et al. [39]. For each 4D-trajectory point (ϕ, λ, h, t), placed in the appropriate cell depending on its coordinates, the separation between this point and all the points in the same and neighbor cells is verified, and if violated, then a point-to-point conflict is detected (see [38] for more details), and the total number of point-to-point conflicts, C_t, is increased. Figure 12 demonstrates the potential conflicts detected for a set of WOFR for 546 eastbound transatlantic flights on July 15^{th} 2012, where the conflict points are marked in red. One can easily see that WOFR are concentrated along a narrow flow which corresponds to the jet stream current. For this reason, the traffic within this flow is highly congested. Thus, strategic conflict resolution becomes important in this case.

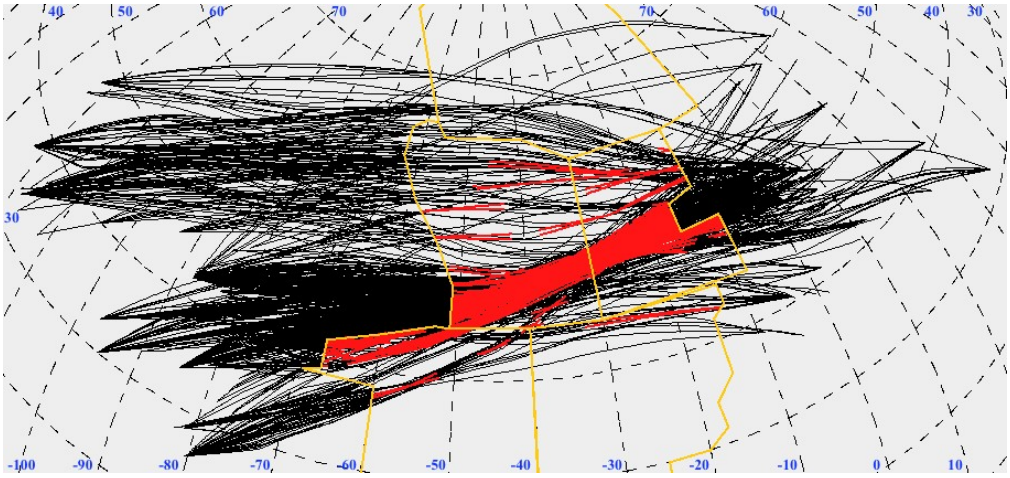

Fig. 12 Potential conflicts detected for WOFR on July 15^{th} 2012

C. Conflict resolution for WOFR

We address the conflict resolution problem as an optimization problem. The input data for this problem are:

- $W(\phi, \lambda, h, t)$- wind fields (4D-grids of W_u and W_v wind coordinates);
- N eastbound WOFR, $f = 1, \ldots, N$,
  - flown at a constant airspeed V^f,
  - and given as a sequence of 4D-route points $q_i^f = (\phi_i^f, \lambda_i^f, h, t_i^f)$

In order to resolve conflicts, we allow two trajectory modification maneuvers: delaying a flight at the departure and shifting a trajectory geometrically. To create a new trajectory for a delayed flight, f, we simply

add a given fixed delay, d^f, to the estimated time, t, at each 4D-point (ϕ, λ, h, t). To comply with Section B, d^f can take integer values from 0 to 20 minutes. Such trajectories remain wind-optimal, as we use static wind fields for the flight time calculation. However, as demonstrated in [20], delaying flights is not enough for conflict resolution, thus, trajectory shape modification is applied. To modify the geometrical shape of a trajectory, we exploit a bijective transformation between an arbitrary curve on a sphere and a curve on the xy-plane, as demonstrated in Figure 13 (see [38], [21] for more details). The bijective function curvature

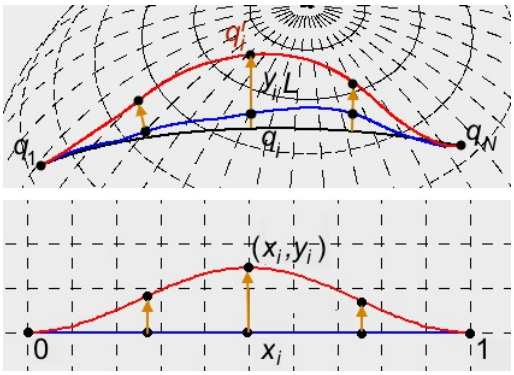

Fig. 13 Trajectory shape modification approach

can be controlled independently for each flight, f, using a single variable, $b^f \in [-1, 1]$. Thus, the vector of decision variables of the optimization problem is given by: $z = (d^1, b^1, ..., d^N, b^N)$, where:

- $d^f \in 0, 1, ..., N^d_{max}$ is the departure time delay of flight f,
- $b^f \in [-1, 1]$ is the rate of trajectory deviation from the initial one for flight f.

The physical constraints of the problem are the separation norms between the 4D trajectory points, which has been relaxed in the objective function as in the previous section III-E. As a result, the only constraints of our formulation are the boundary constraints on the decision variables, and the objective function is designed to minimize the total number of point-to-point conflicts, $C_t(z)$, induced by the set of modified trajectories corresponding to the variables z. In addition to this, we would like to keep the resulting solution as close to the WOFR as possible [21], thus, we penalize trajectory modification maneuvers and include two more terms into the objective function:

- $\Delta T_c(z)$ - total cruising time increase calculated over N flights; and
- $\Delta T_d(z)$ - total departure delays assigned to N flights,

with associated weighting coefficients, α and β. On doing so we obtain the following optimization problem:

$$\begin{aligned} \min_{z} & C_t(z) + \alpha \Delta T_c(z) + \beta \Delta T_d(z), \\ & s.t. d^f \in 0, 1, ..., N^d_{max}, \\ & b^f \in [-1, 1], f = 1, ..., N. \end{aligned} \tag{17}$$

The objective function cannot be explicitly represented in terms of decision variables (d_f, b_f), and has to be evaluated with a simulation process. This problem is therefore a difficult high-dimensional mixed-integer black box (derivative-free) optimization problem. Thus, to resolve it we have chosen to use a standard Simulated Annealing (SA). The basic idea of SA was already presented in Section F. More details on the application of the SA to the conflict resolution af WOFR can be found in[21, 38].

V. Results

This section is divided into two parts. First, results obtained with our new WOTN applied to a real oceanic traffic data are presented. Then, a comparison between the two above-mentioned approaches (WOTN and WOFR) is made. The aim of these simulations is to find better trajectories for a given set of flights and to show the benefits expected from the implementation of the WOTN. Tests were performed with a set of NAT flights selected from the flight plans on $July15^{th}$ 2012 as explained in section II-A.

A. Results with the WOTN

In these simulations, we use the following values for the parameter of the optimization algorithm, which are set empirically:

- The initial temperature $T_{Init} = 0.01$
- The stopping criterion $\beta = 0.0001$,
- The sliding window parameters in minutes: $T_w = 180$, $T_s = 30$.

Several different objective functions were tested. First, we aimed at finding conflict-free trajectories for the considered flights set. Thus, the objective function was defined as: $F^{(1)}_{obj} = C_t$ $(d_1 = c_1 = r_1 = 0)$. The algorithm easily found a **conflict free** solution. Thus, we intended to evaluate the effect of introducing other criteria to the objective function. Here, we focused on the entry delay, D, and the deviation from the desired track, R. Hence, we performed the simulations with the following objective functions:

- $F^{(2)}_{obj} = C_t + 0.1 \times D$
- $F^{(3)}_{obj} = C_t + 0.1 \times R$
- $F^{(4)}_{obj} = C_t + 0.1 \times (D + R)$

Table 3 Result of simulations with different criteria implemented in the objective function

Number of flights	Initial number of conflicts	Objective function	α	Number of Iterations	% of flights with desired entry tracks	% of flights with desired exit tracks	% of flights without delays	Total delays (hours)
546	380	F1	0.95	200	47.9%	49.8%	5.31%	88.4
		F2	0.95	200	54.3%	51.6%	67.7%	17.28
				500	48.7%	49.8%	75.6%	10.5
			0.97	200	50.18%	53.8%	75.4%	12
				500	50.3%	45.6%	82%	9.1
		F3	0.95	200	93.7%	95.9%	4.3%	89.9
				500	95.4%	97%	4.5%	88.6
			0.97	200	94.6%	97%	5.31%	88
				500	96%	97.5%	4.76%	89
		F4	0.95	200	90.2%	94.5%	62%	20.8
				500	93.4%	95.9%	65.9%	17.8
			0.97	200	92.3%	95.7%	65.2%	18.05
				500	***93.4%***	***97%***	***69.41%***	***14.7***

In addition to this, we intended to observe the effect at changing the SA configuration parameters, i.e. the ratio of the temperature decreasing, α, and the number of iteration in each temperature schedule, N. The reference flight set that we used in our simulations contained 546 eastbound flight. Initially, this flight set induced 380 conflict. The most important result is the number of conflict remaining after algorithm executions. Using a basic wind forecast scenario (referred to as s_0 in section B), we were able to obtain a **conflict free** trajectory set with different algorithm configurations. Some results of simulations are shown in Table 3. Based on these simulations, we observe that with the objective function $F_{obj}^{(1)}$, the algorithm performance was poor regarding the number of flights which were assigned their desired tracks and departure times. It is not surprising since these two criteria do not appear in the objective function. The benefits from introducing $F_{obj}^{(2)}$, $F_{obj}^{(3)}$ and $F_{obj}^{(4)}$ are thus clearly seen and the resulting solutions emphasizes the validity of our model.

Another important conclusion that can be made from these results is that the configuration of the SA has a strong effect on the result quality. Increasing the number of iterations, by increasing α and N, for different objective functions increases the number of non-delayed and non-deviated flights. For instance, for the tests with the objective function $F_{obj}^{(2)}$, increasing α from 0.95 to 0.97 and N from 200 to 500 leads to an increase in the number of non-delayed flights from 67% to 82% and to a decrease of the total entry delay from 17 hours to 9 hours (almost by a half).

Comparing the results of tests with $F_{obj}^{(2)}$ and $F_{obj}^{(3)}$ in Table 3, it can be concluded that the two criteria (number of non-delayed flights and number of non-deviated flights) are opposite, and the decrease of the one

Table 4 Comparing results with different objective functions

Objective function	$F_{obj}^{(4)}$	$F_{obj}^{(5)}$	$F_{obj}^{(6)}$
% of flights with desired entry track	93.4%	20%	**89%**
% of flights with desired exit track	97%	8.2%	**92.5%**
% of flights without delay	69.41%	3.85%	**71%**
Total entry delay (hours)	14.7	103	**8.7**
Total cruising time (hours)	3897.379	3829.581	**3855.205**
Average cruising time (hours)	7.13	7	**7.06**

leads to the increase of the other. Hence, the best solution would be a trade-off between these performance criteria. Such a trade-off is achieved with the objective function $F_{obj}^{(4)}$, where the number of deviated and delayed flights are reduced simultaneously. Table 3 shows that the best solution (highlighted in **bold**) is found with the configuration $\alpha = 0.97$ and $N = 500$, and with the objective function $F_{obj}^{(4)}$: Compared to the resulting solution found with $F_{obj}^{(1)}$, the number of flights entering/exiting a desired tracks is increased from 47% to 93% and from 49% to 97% respectively, and the number of non-delayed flights is increased from 5.3% to 69.4%, leading to a significant decrease in the total entry delay from 88.4 hours to 14.7 hours.

These encouraging results motivated us to explore other performance criteria. Thus, further we focused on investigating the potential benefits from including the total cruise time into the objective function. More simulations are performed using the following objective functions:

- $F_{obj}^{(4)} = C_t + 0.1 \times (D + R)$
- $F_{obj}^{(5)} = C_t + 0.1 \times C$
- $F_{obj}^{(6)} = C_t + 0.1 \times (C + D + R)$

The obtained results are summarized in Table 4. In these simulations, we set $\alpha = 0.97$ and $N = 500$. With the objective function $F_{obj}^{(5)}$, we minimized cruising time only, and obtained the reduction in the total cruising time of approximately 70 hours. These time savings come from attributing to the aircraft tracks with preferable winds. However, using $F_{obj}^{(5)}$ has a negative impact on the number of non-delayed and non-deviated flights: the number of non-deviated flights is decreased up to 8%, and the number of non-delayed flights is about 4%. Thus, comparing results from Table 4, we conclude that the best trade-off is given by the objective function $F_{obj}^{(6)}$ (highlighted in **bold**), taking into account all the criteria. The total cruising time across the set of all flights during July 15 is decreased by almost 40 hours when applying the objective function $F_{obj}^{(6)}$ compared to the total cruising time found with the objective function $F_{obj}^{(4)}$, without dramatic influence on the other criteria of the objective function. We believe this is a very satisfying solution that proves the effectiveness of our algorithm. Based on this solution, further analysis was performed in order to prove the benefits from using wind-optimal tracks.

Table 5 Cruise time for WOTN flights compared to WOFR flights

Cruise time decrease	Less than 5 minutes	19.4 %
	Between 5 and 10 minutes	3.6 %
Cruise time increase	Less than 10 minutes	37 %
	Between 10 and 30 minutes	20 %
	Between 30 minutes and 1 hour	14.5 %
	More than 1 hour	5.5 %

To do so, we compared the obtained cruising times along the WOTN with the corresponding cruising times along great circle routes. The great-circle distance is the shortest distance between the two points on the Earth surface. In our case, it represented the shortest distance between the entry track way-point and the exit track way-point for each flight. Obviously, the great-circle trajectory length is shorter than the corresponding trajectory obtained using the WOTN. However, we were interested in comparing the cruising times when following wind-optimal tracks and great-circle routes. Simulations showed that all flights in the considered flight set decreased their cruising times when using wind-optimal tracks compared to the great-circle routes. Moreover, about 76.5% of flights decreased their cruising times by the values from 30 to 53 minutes. Knowing that flights spend on average about 4 hours in the WOTN, we conclude that 76.5% of flights gained more than 12.5% from their total cruising time in the NAT airspace. Thus, we observed that flights can cross the NAT airspace faster, even following longer trajectories. Clearly, this is due to using trajectories with preferable winds.

The next section focuses on comparing wind-optimal trajectories WOFR, discussed in Section IV, to the WOTN presented in Section III.

B. Comparison between WOFR and WOTN structure

In this section, we compare the two approaches of the traffic organization: wind-optimal free routes WOFR and wind-optimal track network WOTN. The explicit results of conflict resolution using wind optimal trajectories can be found in [21, 28]. Here we test both algorithms on the same data set (546 eastbound flights on July $15th$ 2012). First, we reveal the difference in the cruising times along the trajectories obtained using the two approaches. Next, we evaluate the robustness of these trajectories under changing winds.

Cruising times evaluation: Here we compare the best solution based on the WOTN described in the previous section V-A (highlighted in **bold** in Table 4) with the solution resulting from the conflict resolution with WOFR. Results are summarized in Table 5.

Our simulations revealed that almost 23% of flights reduce their cruising times when using the WOTN

compared to using WOFR. The gain in cruising time when using WOTN compared to WOFR does not exceed 10 minutes, and only 3.6% of flights gain more than 5 minutes. The fact that the conflict resolution algorithm based on WOFR yielded greater cruising times for some flights comes from the nature of conflict resolution maneuvers: when the trajectory shape is modified, the resulting trajectory is no longer wind-optimal, and in some cases, this leads to important cruising time increase. The rest of flights (about 77%) have greater cruising times when following the WOTN compared to their trajectories using WOFR. For about 57% of flights the difference in cruising times is less then 30 minutes, while the rest 20% of flights extend their travel times by more than 30 minutes. This is not particularly surprising, as WOFR are constructed independently for each single flight based on its characteristics. However, we observed that for about 80% of flights possible increase in cruising time when using WOTN compared to WOFR is less than 30 minutes, while for 60% of flights this increase is less than 10 minutes. We thus conclude that the proposed WOTN yields efficient routes for the majority of flights.

At the same time, we found out that for about 5.5% of flights, their cruising times are increased by more than one hour when following WOTN compared to WOFR. This issue can be explained by the fact that the location of the wind-optimal tracks is basically around latitude 50°(by construction), and thus flights departing from the north of the USA (around latitude 60°) and heading to the north of Europe (keeping almost the same latitude 60°), as well as flights departing from the south of the USA (around latitude 30°) and heading to the south of Europe (around latitude 40°), receive significant extension to their trajectories when using the WOTN.

Robustness evaluation: In this section, we evaluate the robustness of the two obtained solutions based on WOFR and WOTN under wind uncertainties. To do so, we performed the conflict resolution with the two approaches using the nominal forecast wind, denoted $s0$ (refer to Section II-B), and then we re-evaluated the resulting solutions with different wind scenarios. Tests were performed with the 4 different wind scenario ($s1$, $s2$, $s3$ and $s4$) described in section II-B. The results are summarized in Table 6. From these results we observe

Table 6 Comparing results with different wind scenarios

	Initial nb. of conflicts	Residual conflicts	Residual conflicts with scenarios:			
			s1	s2	s3	s4
Wind-optimal trajectories	307	0	92	106	135	159
WOTN	380	0	16	22	10	5

that when the conflict resolution approach based on WOFR is used, a big number of conflicts reappear once

the conflict-free trajectory set is evaluated in different wind fields. With the wind scenario $s4$, the number of reappeared conflicts is about 159 which represents almost 50% of the initial number of conflicts. On the other hand, when the conflict resolution approach based on the WOTN is used, the number of reappeared conflicts is significantly lower, i.e. it does not exceed 22. Thus, we conclude that the WOTN is much more robust regarding the wind changes than a set of individual WOFR, which is particularly important for the strategic planning involving important uncertainties.

Conclusions

In this paper, two approaches for scheduling transatlantic flights at the strategic level of flight planning are presented. The first approach is based on a route structure, Wind-Optimal Track Network (WOTN), that benefits from the jet stream direction, while the second one is based on wind-optimal free routes (WOFR). WOTN represents a set of predefined tracks where flights are required to follow these tracks, while WOFR allow flight to choose their specific trajectories independently from the others.

The paper describes the optimization algorithms implemented for each of the approaches aimed at improving flight routes and reducing the associated congestion, delays and cruising times. Simulations were performed on real North Atlantic traffic data under the assumption of reduced separation norms, and the obtained optimized trajectories were compared.

The performed simulations demonstrated that both algorithms were able to find conflict-free trajectory configurations under the reduced separation norms. Moreover, the results revealed strong benefits from flying wind-optimal routes in North Atlantic airspace. Indeed, almost 76.5% of flights decreased their cruising times by the value from 30 to 53 minutes when flying wind-optimal trajectories compared to using great circle trajectories. Furthermore, by comparing the two approaches, we conclude that flying WOFR leads to better results in term of cruising times than using the WOTN. However, the WOTN was found to be much more robust in terms of the number of conflicts that reappear when considering wind changes.

Thus, our research highlights the importance of taking advantages from the favorable winds in order to decrease the flight cruising times, on the one hand, and the importance of implementing a route structure in order to increase the robustness under wind uncertainties, on the other hand.

Acknowledgments

The work on developing the conflict resolution algorithm for wind-optimal trajectories was partly performed under an appointment to the NASA Postdoctoral Program at NASA Ames Research Center, administrated by Universities Space Research Association through a contract with NASA. The authors would like to gratefully acknowledge Dr. Banavar Sridhar and Dr. Hok K. Ng from NASA Ames Research Center for providing the

data on the transatlantic flights and designing the wind-optimal trajectories.

References

[1] European, and of ICAO, N. A. O., *North Atlantic operations and airspace manual-NAT Doc 007*, International Civil Aviation Organization (ICAO), 2018.

[2] Kerczewski, R. J., Greenfeld, I., and Welch, B. W., "Communications, navigation and surveillance for improved oceanic air traffic operations," *2005 IEEE Aerospace Conference*, 2005, pp. 1799–1805. doi:10.1109/AERO.2005.1559472.

[3] Foundation, F. S., "Benefits Analysis of Space-Based ADS-B," Flight Safety Foundation, 2016.

[4] Craig Foster, V. C., Senior Consultant, "Aircraft Surveillance Versus Tracking," VALOUR CONSULTANCY, 2016.

[5] Administration, T. F. A., "Enhanced Surveillance Capabilities in FAA Controlled Oceanic Airspace: Operational Need and Added Benefits," RTCA, 2017.

[6] *Use of Automatic Dependent Surveillance-Broadcast (ADS-B) Out in Support of Reduced Vertical Separation Minimum (RVSM) Operations*, Federal Aviation Administration (FAA), Department of Transportation (DOT), 2017.

[7] Williams, A., Mondoloni, S., Western, R., Karakis, T., and Jones, K., "Beneficial Applications of Airborne Separation Assurance Systems (ASAS) in the Southern Pacific Airspace," *AIAA 5th ATIO and16th Lighter-Than-Air Sys Tech. and Balloon Systems Conferences, Aviation Technology, Integration, and Operations (ATIO) Conferences, American Institute of Aeronautics and Astronautics*, 2005. doi:10.2514/6.2005-7337.

[8] Williams, A., and Greenfeld, I., "Benefits assessment of reduced separations in North Atlantic Organized Track System," *6th AIAA Aviation Technology, Integration and Operations Conference (ATIO)*, 2006, p. 7816. doi:10.2514/6.2006-7816.

[9] Rodionova, O., Sbihi, M., Delahaye, D., and Mongeau, M., "Optimization of aicraft trajectories in North Atlantic oceanic airspace," *ICRAT 2012, 5th International Conference on Research in Air Transportation*, Berkeley, United States, 2012. URL `https://hal-enac.archives-ouvertes.fr/hal-00938895`.

[10] Rodionova, O., Sbihi, M., Delahaye, D., and Mongeau, M., "North Atlantic Aircraft Trajectory Optimization," *IEEE Transactions on Intelligent Transportation Systems*, Vol. 15, IEEE, 2014, pp. pp 2202–2212. doi:10.1109/TITS.2014.2312315, URL `https://hal-enac.archives-ouvertes.fr/hal-00981337`.

[11] Girardet, B., Lapasset, L., Delahaye, D., and Rabut, C., "Wind-optimal path planning: Application to aircraft trajectories," *2014 13th International Conference on Control Automation Robotics Vision (ICARCV)*, 2014, pp. 1403–1408. doi:10.1109/ICARCV.2014.7064521.

[12] Patron, R. F., Kessaci, A., Botez, R. M., and Labour, D., "Flight trajectories optimization under the influence of winds using genetic algorithms," *AIAA Guidance, Navigation, and Control (GNC) Conference*, 2013, p. 4620. doi:10.2514/6.2013-4620.

[13] Ng, H. K., Sridhar, B., and Grabbe, S., "A practical approach for optimizing aircraft trajectories in winds," *2012 IEEE/AIAA 31st Digital Avionics Systems Conference (DASC)*, 2012, pp. 3D6–1–3D6–14. doi:10.1109/DASC.2012.6382319.

[14] Irvine, E. A., Hoskins, B. J., Shine, K. P., Lunnon, R. W., and Froemming, C., "Characterizing North Atlantic weather patterns for climate-optimal aircraft routing," *Meteorological Applications*, Vol. 20, 2013, pp. 80–93. doi:10.1002/met.1291, URL `https://rmets.onlinelibrary.wiley.com/doi/abs/10.1002/met.1291`.

[15] Grabbe, S., Sridhar, B., and Cheng, N., "Central east pacific flight routing," *Air Traffic Control Quarterly*, Vol. 15, 2007, pp. 239–264. doi:10.2514/atcq.15.3.239.

[16] Ng, H. K., Sridhar, B., Grabbe, S., and Chen, N., "Cross-polar aircraft trajectory optimization and the potential climate impact," *2011 IEEE/AIAA 30th Digital Avionics Systems Conference*, 2011, pp. 3D4–1–3D4–15. doi:10.1109/DASC.2011.6096060.

[17] E., B. A., and Ho, Y. C., *Applied Optimal Control Taylor and Francis Levittown PA*, Vol. 2, 1975.

[18] Sridhar, B., Ng, H. K., Linke, F., and Chen, N. Y., "Benefits analysis of wind-optimal operations for trans-atlantic flights," *14th AIAA Aviation Technology, Integration, and Operations Conference, AIAA paper, vol. AIAA*, Vol. 2583, 2014, pp. 1–12. doi:10.2514/6.2014-2583.

[19] Grabbe, S., Sridhar, B., and Mukherjee, A., "Central East Pacific flight scheduling," *AIAA Guidance, Navigation, and Control Conference and Exhibition*, 2007. doi:10.2514/6.2007-6447.

[20] Sridhar, B., Chen, N. Y., Hok, K. N., Rodionova, O., Delahaye, D., and Linke, F., "Strategic Planning of Efficient Oceanic Flights," *ATM seminar 2015, 11th USA/EUROPE Air Traffic Management R&D Seminar*, FAA & Eurocontrol, Lisboa, Portugal, 2015. URL `https://hal-enac.archives-ouvertes.fr/hal-01168653`.

[21] Rodionova, O., Delahaye, D., Sridhar, B., and Ng, H. K., "Deconflicting wind-optimal aircraft trajectories in North Atlantic oceanic airspace," *AEGATS 16, Advanced Aircraft Efficiency in a Global Air Transport System*, AAF, Paris, France, 2016. URL `https://hal-enac.archives-ouvertes.fr/hal-01304633`.

[22] Dhief, I., Dougui, N. H., Delahaye, D., and Hamdi, N., "Strategic planning of aircraft trajectories in North Atlantic oceanic Airspace based on flocking behaviour," *IEEE Congress on Evolutionary Computation (CEC)*, 2016. doi:10.1109/CEC.2016.7744091.

[23] Dey, C., *GRIB (Edition 1)*, The WMO format for the storage of weather product information and the exchange of weather product messages in gridded binary form as used by NCEP central operations, U.S. Department of

Commerce, National Oceanic and Atmospheric Administration, National Weather Service, National Centers for Environmental Prediction, office Note 388, 1998.

[24] Gneiting, T., and Raftery, A. E., "Weather forecasting with ensemble methods," *Science*, Vol. 310, American Association for the Advancement of Science, 2005, pp. 248–249. doi:10.1126/science.1115255.

[25] Palmer, T. N., "The economic value of ensemble forecasts as a tool for risk assessment: From days to decades," *Quarterly Journal of the Royal Meteorological Society*, Vol. 128, 2002, pp. 747–774. doi:10.1256/0035900021643593, URL `https://rmets.onlinelibrary.wiley.com/doi/abs/10.1256/0035900021643593`.

[26] Sloughter, J. M., Gneiting, T., and Raftery, A. E., "Probabilistic Wind Speed Forecasting Using Ensembles and Bayesian Model Averaging," *Journal of the American Statistical Association*, Vol. 105, No. 489, 2010, pp. 25–35. doi:10.1198/jasa.2009.ap08615, URL `https://doi.org/10.1198/jasa.2009.ap08615`.

[27] Rivas, D., Vazquez, R., and Franco, A., "Probabilistic Analysis of Aircraft Fuel Consumption Using Ensemble Weather Forecasts," *7th International Conference on Research in Air Transportation (ICRAT), Philadelphia, PA*, 2016, pp. 1–8.

[28] Rodionova, O., Sridhar, B., and Ng, H. K., "Conflict resolution for wind-optimal aircraft trajectories in North Atlantic oceanic airspace with wind uncertainties," *2016 IEEE/AIAA 35th Digital Avionics Systems Conference (DASC)*, 2016, pp. 1–10. doi:10.1109/DASC.2016.7778010.

[29] Legrand, K., Puechmorel, S., Delahaye, D., and Zhu, Y., "Aircraft trajectory planning under wind uncertainties," *2016 IEEE/AIAA 35th Digital Avionics Systems Conference (DASC)*, 2016, pp. 1–9. doi:10.1109/DASC.2016.7777955.

[30] Hwang, C.-R., "Simulated annealing: Theory and applications," *Acta Applicandae Mathematica*, 1988. doi:10.1007/BF00047572.

[31] Kirkpatrick, S., Gelatt, C. D., and Vecchi, M. P., "Optimization by Simulated Annealing," *Science*, Vol. 220, No. 4598, 1983, pp. 671–680. doi:10.1126/science.220.4598.671, URL `http://science.sciencemag.org/content/220/4598/671`.

[32] Viets, K. J., and Ball, C. G., "Validating a future operational concept for en route air traffic control," *IEEE Transactions on Intelligent Transportation Systems*, Vol. 2, 2001, pp. 63–71. doi:10.1109/6979.928717.

[33] Kirk, D. B., Heagy, W. S., and Yablonski, M. J., "Problem resolution support for free flight operations," *IEEE Transactions on Intelligent Transportation Systems*, Vol. 2, 2001, pp. 72–80. doi:10.1109/6979.928718.

[34] Andresson, E. I., "Lateral Optimization of Aircraft Tracks in Reykjavik Air Traffic Control Area," Ph.D. thesis, School of Science and Engineering, Reykjavik University, Mai 2012. URL `http://hdl.handle.net/1946/12682`.

[35] Wickramasinghe, N. K., Harada, A., and Miyazawa, Y., "Flight trajectory optimization for an efficient air transportation system," *28th Congress of the International Council of the Aeronautical Sciences ICAS*, Vol. 6, 2012, pp. 4399–4410.

[36] Ng, H. K., Sridhar, B., Chen, N. Y., and Li, J., "Three-dimensional trajectory design for reducing climate impact of Trans-Atlantic flights," *14th AIAA Aviation Technology, Integration, and Operations Conference, AIAA paper, vol. AIAA*, 2014. doi:10.2514/6.2014-2289, URL `https://doi.org/10.2514/6.2014-2289`.

[37] Grewe, V., Matthes, S., Frömming, C., Brinkop, S., Jöckel, P., Gierens, K., Champougny, T., Fuglestvedt, J., Haslerud, A., Irvine, E., and Shine, K., "Feasibility of climate-optimized air traffic routing for trans-Atlantic flights," *Environmental Research Letters*, Vol. 12, No. 3, 2017. doi:10.1088/1748-9326/aa5ba0, URL `http://centaur.reading.ac.uk/69316/`.

[38] Rodionova, O., "Aircraft trajectory optimization in North Atlantic oceanic airspace," Theses, Université Paul Sabatier - Toulouse III, Jun. 2015. URL `https://tel.archives-ouvertes.fr/tel-01214990`.

[39] Chaimatanan, S., Delahaye, D., and Mongeau, M., "A Hybrid Metaheuristic Optimization Algorithm for Strategic Planning of 4D Aircraft Trajectories at the Continental Scale," *IEEE Computational Intelligence Magazine*, Vol. 9, 2014, pp. 46–61. doi:10.1109/MCI.2014.2350951.